HHS Public Access

Author manuscript

Clin Cancer Res. Author manuscript; available in PMC 2017 September 01.

Published in final edited form as:

Clin Cancer Res. 2016 September 1; 22(17): 4328–4340. doi:10.1158/1078-0432.CCR-15-3026.

Blocking Indolamine-2,3-Dioxygenase Rebound Immune Suppression Boosts Anti-tumor Effects of Radio-Immunotherapy in Murine Models and Spontaneous Canine Malignancies

Arta M. Monjazeb[1,*], **Michael S. Kent**[2], **Steven K. Grossenbacher**[3], **Christine Mall**[3], **Anthony E. Zamora**[3], **Annie Mirsoian**[3], **Mingyi Chen**[4], **Amir Kol**[5], **Stephen L. Shiao**[6], **Abhinav Reddy**[1], **Julian R. Perks**[1], **William Culp**[2], **Ellen E. Sparger**[2], **Robert J. Canter**[7], **Gail D. Sckisel**[3], and **William J. Murphy**[3,8]

[1]Department of Radiation Oncology, UC Davis Comprehensive Cancer Center, Sacramento, CA 95817, USA

[2]Department of Surgical and Radiological Sciences, UC Davis School of Veterinary Medicine, Davis, CA 95616, USA

[3]Department of Dermatology, UC Davis Health Sciences, Sacramento, CA 95817, USA

[4]Department of Pathology, UC Davis Health Sciences, Sacramento, CA 95817, USA

[5]Department of Pathology, Microbiology, and Immunology, UC Davis School of Veterinary Medicine, Davis, CA 95616, USA

[6]Departments of Radiation Oncology and Biomedical Sciences, Cedars-Sinai Medical Center, Los Angeles, CA 90048, USA

[7]Department of Surgery, Division of Surgical Oncology, UC Davis Comprehensive Cancer Center, Sacramento, CA 95817, USA

[8]Department of Internal Medicine, Division of Hematology and Oncology, UC Davis Comprehensive Cancer Center, Sacramento, CA 95817, USA

Abstract

Purpose—Previous studies demonstrate that intratumoral CpG immunotherapy in combination with radiotherapy acts as an *in-situ* vaccine inducing anti-tumor immune responses capable of eradicating systemic disease. Unfortunately, most patients fail to respond. We hypothesized that immunotherapy can paradoxically up-regulate immunosuppressive pathways, a phenomenon we

[*]To whom correspondence should be addressed: Arta M. Monjazeb, M.D., Ph.D., Department of Radiation Oncology, UC Davis Comprehensive Cancer Center, Sacramento, CA 95817, USA, ammonjazeb@ucdavis.edu.

Conflict of interest statement: The authors disclose no potential conflicts of interest

Author contributions

A. M.M. designed and carried out experiments and canine clinical trial, analyzed and interpreted data, and prepared manuscript for submission. M. S. K., W.C., and E. E.S. helped design and perform canine clinical trial, and analyze and interpret data from canine clinical trial. S.K.G., C.M., A. E.Z., A.M., A. R., and G.D.S. performed experiments, analyzed data, and helped with manuscript preparation. M.C. analyzed and interpreted immunohistochemistry. A.K. stained, analyzed, and interpreted immunofluorescence. S.L.S. performed macrophage polarization studies and helped with manuscript preparation. J.R. P. performed quality assurance and physics calculations for mouse irradiation. R.J.C. assisted with data interpretation and manuscript preparation. W.J.M. assisted with experimental design, data interpretation, and manuscript preparation.

term “rebound immune suppression”, limiting clinical responses. We further hypothesized that the immunosuppressive enzyme indolamine-2,3-dioxygenase (IDO) is a mechanism of rebound immune suppression and that IDO blockade would improve immunotherapy efficacy.

Experimental Design—We examined the efficacy and immunologic effects of a novel triple therapy consisting of local radiotherapy, intratumoral CpG, and systemic IDO blockade in murine models and a pilot canine clinical trial.

Results—In murine models we observed marked increase in intra-tumoral IDO expression after treatment with radiotherapy, CpG or other immunotherapies. The addition of IDO blockade to radiotherapy + CpG decreased IDO activity, reduced tumor growth, and reduced immunosuppressive factors, such as regulatory T-cells (Tregs) in the tumor microenvironment. This triple combination induced systemic anti-tumor effects, decreasing metastases and improving survival in a CD8+ T-cell dependent manner. We evaluated this novel triple therapy in a canine clinical trial, since spontaneous canine malignancies closely reflect human cancer. Mirroring our mouse studies, the therapy was well tolerated, reduced intra-tumoral immunosuppression, and induced robust systemic anti-tumor effects.

Conclusion—These results suggest that IDO maintains immune suppression in the tumor after therapy and IDO blockade promotes a local anti-tumor immune response with systemic consequences. The efficacy and limited toxicity of this strategy are attractive for clinical translation.

Keywords

radiotherapy; immunotherapy; indolamine-2,3-dioxygenase; CpG; Treg

Introduction

Immunotherapy is revolutionizing metastatic cancer therapy. Patients responding to these therapies can achieve durable long-term remissions. However, most patients fail to respond, and some can experience significant immune-mediated toxicities (1–3). There is growing interest in understanding mechanisms of resistance to immunotherapy and finding combinatorial strategies to further increase efficacy while minimizing toxicity. Local radiotherapy (RT) is an ideal candidate for combined modality immunotherapy strategies. In addition to debulking tumor and releasing tumor antigens, RT has well-established immunomodulatory effects (4). Preclinical and clinical reports confirm the safety and efficacy of multimodality strategies employing RT and immunotherapy. One particularly promising strategy is RT in combination with the immune stimulatory toll-like receptor 9 (TLR9) agonist CpG oligodeoxynucleotide (CpG), which has demonstrated significant synergy in pre-clinical models (5) and the ability to induce regression of systemic disease in clinical trials (6, 7). Systemic response rates were about 20% with disease stability in another 20% of patients with refractory systemic (6) or cutaneous lymphoma (7). However, patients whose tumors induced Tregs responded poorly. The effects of CpG on Treg mediated immune suppression can be paradoxical. CpG can reduce Tregs by converting them to a T-helper phenotype via IL-6 production (8) and can also directly reverse Treg

function (9). Conversely, CpG can directly induce Foxp3 expression (10) and up-regulate indolamine-2,3-dioxygenase (IDO) (8) which is known to induce and maintain Tregs.

IDO is an immunosuppressive enzyme that catalyzes the rate-limiting step in the catabolism of tryptophan to kynurenine and is expressed by numerous human malignancies (11, 12). IDO expression can induce immune tolerance to malignancies (13) via complex mechanisms (14). In dendritic cells IDO can activate Treg suppressive function in a CTLA-4 dependent manner (15). It can also prevent dendritic cell IL-6 production, thereby preventing Treg conversion and maintaining elevated Treg levels despite inflammatory signals such as CpG (16). Furthermore, IDO can directly induce Tregs from naïve CD4+ T cells via 3-hydroxyanthranillic acid, a downstream catabolite of IDO tryptophan metabolism (17, 18). IDO can, through similarly complex mechanisms, inhibit natural killer cells and prevent effector T-cell activation and proliferation (14, 19). IDO expression can be paradoxically upregulated after inflammatory signals(20, 21) presumably as a mechanism to limit inflammation and maintain immune homeostasis. 1-Methyl -Tryptophan (1MT) is a pharmacologic inhibitor of IDO with demonstrated anti-tumor properties which is being tested alone or in combination with chemotherapy in human trials (22).

Using a novel immunotherapy strategy combining local RT, intratumoral CpG, and IDO blockade, we tested the hypothesis that IDO upregulation after immunostimulatory therapies, such as RT + CpG, maintains tumor microenvironment immune suppression and limits treatment efficacy. We show that immunostimulatory therapies paradoxically up-regulated IDO expression, which we termed “rebound immune suppression”. The addition of 1MT decreased IDO activity, decreased Tregs and other immune suppressive factors within the tumor, and significantly improved the anti-tumor effects of RT + CpG in a CD8+ T-cell dependent manner. Although the immune effects were primarily limited to the microenvironment of the treated tumor, systemic anti-tumor responses were observed. We confirmed these results in a veterinary clinical trial of companion canines since canine cancers closely represent human malignancy. We observed significant responses at the RT treated primary tumor as well as at untreated sites of metastatic disease in most dogs. There were also significant changes in the immunosuppressive tumor micro-environment, corroborating our mechanistic mouse data. In marked contrast to immune checkpoint inhibitors, little toxicity was observed in mouse or canine studies. These results confirm the potency of combinatorial immunotherapy strategies and suggest that IDO may play a critical role in maintaining the immunosuppressive tumor microenvironment after immunotherapy. The addition of IDO blockade may safely improve the efficacy of immunotherapy by preventing rebound immune suppression.

Materials and Methods

In Vivo Reagents

CpG ODN 1826 (mouse studies) and 2006 (canine studies) were purchased from Invivogen. 1-methyl-D,L-tyrptophan was purchased from Sigma-Aldrich. CD8 depleting antibody (cloneYTS169.4) was administered prior to the start of therapy and once weekly thereafter. The agonistic anti-mouse CD40 antibody (FGK115.B3) was generated as previously described (23). Rat IgG (Jackson ImmunoResearch Laboratories) was used as a control for

anti-CD40. Recombinant human interleukin-2 (rhIL2; Teceleukin, Roche) was provided by the National Cancer Institute (NCI).

Mouse tumor studies

All studies were approved by the UC Davis IACUC and human endpoints were used. Female 8- to 12-week-old C57BL/6 or BALB/c mice were purchased from the animal production area at the NCI. All mice were housed at the UC Davis animal facilities under specific-pathogen-free conditions. Mouse tumor studies were performed as outlined (Figure 1D). 4T1 breast adenocarcinoma tumors were grown orthotopically in the mammary fat pad of BALB/c mice and B16 melanoma tumors were implanted into the flank of C57BL/6 mice. Mouse tumors were irradiated with 8 Gy per fraction delivered with 9MeV electrons on an Elekta synergy clinical accelerator using a 2cm diameter electron field and 0.5 cm bolus. Treatment accuracy was confirmed using anthropomorphic phantoms as previously described (24). Mice were sacrificed and tissues harvested at 7 or 14 days post treatment completion for mechanistic studies.

Canine clinical Trial

This clinical trial was approved by the UC Davis School of Veterinary Medicine Clinical Trials Review Board and IACUC. Five canines with histologically confirmed metastatic melanoma or sarcoma were enrolled with informed consent of their owners. The trial schema is outlined in supplemental Figure 1. Treatment consisted of weekly 8 Gy fractions of radiotherapy repeated for a total of four treatments over 4 weeks. Radiotherapy was delivered to the primary tumor only using a clinical grade linear accelerator at the UC Davis Center for Companion Animal Health. After each radiotherapy treatment, canines received a 2mg intratumoral injection of CpG. Patients also received oral 1MT at 1200mg daily for the 28 day treatment period. Radiologic scans, blood and tissue samples were obtained pre-treatment and at follow up visits at weeks 5, 8, and 20. Radiographic response rates were determined using irRECIST criteria (25). Patients were evaluated by a veterinary radiation oncologist for treatment toxicity weekly during therapy and at the 5, 8, and 20 week follow-up visits using clinical exam and blood labs. Toxicity was graded according to the VRTOG criteria (26).

Flow Cytometry

Staining procedures and antibodies are detailed in supplemental methods. All data were collected using a BD Fortessa flow cytometer equipped with BD FACSDiva software. Data were analyzed using FlowJo v10 (TreeStar).

Quantitative Real Time PCR (qRT-PCR)

Quantitative real-time PCR was performed using AB Step-ONE Plus (Applied Biosystems) in the presence of SYBR Green Supermix (Applied Biosystems). Details of RNA isolation, cDNA synthesis, and qRT-PCR can be found in supplemental methods.

Kynurenine / Tryptophan ratio

Kynurenine to tryptophan ratio was determined using mass spectrometry at the UC Davis Metabolomics Center as detailed in supplemental methods.

Statistics

Statistical analysis was performed with Prism software (GraphPad). Data were expressed as mean ± SEM. For analysis of three or more groups, the one-way ANOVA was performed with the Holm-Sidak correction for multiple comparisons. Analysis of differences between two normally distributed test groups was performed with the Student's t test. Welch's correction was applied to Student's t test datasets with significant differences in variance. *$p < 0.05$, **$p < 0.01$, *** $p < 0.001$, ****$p < 0.0001$.

Immunofluorescence and Immunohistochemistry methods are detailed in supplemental methods.

Results

IDO upregulation in the tumor microenvironment after immunostimulatory therapies

To test our hypothesis that IDO mediated "rebound immune suppression" maintains immune suppression and limits treatment efficacy, we employed the poorly immunogenic and highly metastatic mouse 4T1 orthotopic breast tumor model (27). We first evaluated IDO expression within the tumor microenvironment after immunostimulatory therapies and observed a significant increase in IDO expressing cells compared to untreated controls in the glandular nests of malignant cells (Figure 1A–B, $p<0.0001$). IDO can be upregulated by tumor infiltrating immune cells as well as tumor cells. In our model, IDO upregulation appears to be predominately in the neoplastic epithelial cells. IDO upregulation within 4T1 cells was verified *in-vitro* as well (data not shown). We likewise observed a parallel statistically significant 3- to 5-fold increase in IDO mRNA expression (Figure 1C). Importantly, this upregulation of IDO was not limited to RT and CpG but was also observed with other immunotherapy strategies (Figure 1A–C). These results indicate that immunotherapy can paradoxically upregulate immunosuppressive pathways, such as IDO, which may limit efficacy.

Systemic 1MT significantly decreases IDO activity and augments the anti-tumor efficacy of local RT + CpG

To investigate if IDO mediated "rebound immune suppression" after RT + CpG limits treatment efficacy we next tested the effects of adding systemic IDO blockade. Our treatment schema (Figure 1D) consisted of two 8 Gy fractions of local RT administered to the primary tumor over a 7 day period. Each fraction of RT was accompanied by intratumoral injection of 20 ug of CpG based on dose response data. CpG was administered locally to mirror human clinical trials and minimize systemic toxicity (6, 7). For IDO blockade, 1MT was administered by daily 2 mg i.p. injections throughout the study period. The triple combination decreased IDO enzymatic activity, as measured by serum kynurenine / tryptophan ratio, below the level of untreated controls (Figure 1E, $p=0.03$). We next evaluated the anti-tumor effects of 1MT, RT, and CpG, alone or in combination. CpG

and 1MT alone or in combination had no significant effect on tumor growth (Figure 1F). Local RT alone significantly reduced tumor growth but by day 34 there was accelerated tumor outgrowth and mean tumor size was no longer statistically different than controls (Figure 1F, G). Although CpG and 1MT had no anti-tumor effects alone or in combination, when either one was combined with RT they significantly inhibited tumor growth (Figure 1F, G). Notably, the triple combination was significantly better than either RT + CpG or RT + 1MT decreasing tumor growth by an additional 3-fold (Day 34 mean tumor size: 377 mm^3, 1060 mm^3, 1057mm^3, respectively; Figure 1F). The triple therapy also significantly improved the survival of 4T1 bearing mice (Figure 1H, $p<0.001$). To ensure these results were not tumor or mouse strain specific, we tested this regimen in C57BL/6 mice bearing B16 melanoma tumors. Again, mice treated with the triple combination had significantly smaller tumors than mice treated with RT + CpG (Figure 1I, $p=0.042$). Importantly, in both models there was no evidence of autoimmune or other toxicities induced by the therapy. Thus, as hypothesized, the addition of 1MT significantly improved the anti-tumor effects of RT + CpG in 4T1 and B16 tumors (Figure 1G, I).

We next examined the systemic anti-tumor effects of this triple therapy in 4T1 bearing mice. At day 40 heavy burdens of pulmonary metastatic disease could be grossly identified in control but not treated mice (Figure 1J). The primary tumors (located in the distal mammary fat pad) were treated with 2cm radiation portals and the lungs were well outside of the radiation fields. Similar results were also observed by computed tomography (CT) imaging (Figure 1K) and further corroborated in quantifiable fashion using *in-vitro* lung tumor colony forming assays with a 6-fold reduction in lung colony forming units in the triple combination group compared to controls at day 28 (Figure 1L, $p=0.001$). Crucially, lungs from the majority of the triple combination treated mice grew no tumor colonies.

Taken together, our findings indicate that RT + CpG resulted in anti-tumor effects but also upregulated IDO expression. The addition of IDO blockade with 1MT decreased IDO activity and significantly improved the anti-tumor effects. This triple therapy was well tolerated, increased survival, and markedly reduced systemic metastases.

RT + CpG + 1MT induces systemic anti-tumor effects in spontaneous canine malignancies

Based on our murine studies, we initiated a pilot clinical trial for outbred companion canines with spontaneous metastatic melanomas and sarcomas. Due to the aggressive nature and poor prognosis of these cancers, the standard of care for these canine patients is palliative RT to the primary tumor consisting of 4 weekly fractions of 8 Gy. Our treatment protocol (supplemental Figure 1A) built on this palliative regimen but mirrored our mouse studies with an intratumoral injection of CpG at the time of RT and daily administration of 1MT for the treatment course. CpG was administered at 2 mg/dose to mirror human clinical studies. The activity of CpG ODN 2006 used in human clinical trials was verified in canines with an *in-vitro* peripheral blood mononuclear cell (PBMC) proliferation assay (supplemental Figure 1B). 1MT was administered orally at 1200 mg per day based on pharmacokinetic studies in canines (28). We verified the ability of 1MT to reduce IDO enzymatic activity in canines by measuring serum kynurenine / tryptophan ratio in samples collected from trial canines (supplemental Figure 1C, $p=0.02$). We enrolled 5 canines with rapidly progressing

metastatic disease to this pilot trial (Supplemental Table 1). Four had mucosal melanomas with pulmonary metastases and one had soft tissues sarcoma with nodal and pulmonary metastases (Supplemental Table 1). Canines with metastatic melanomas have an extremely poor prognosis (29). The survival of canines in this study (5.8 months, 95% CI: 3.2– 9.2 months) exceeded published historical controls (29). All 5 canines responded at the primary site of disease which was within the radiation portals (Supplemental Table 1, Figure 2A–D). The local response to therapy was robust with a 50–100% reduction in tumor mass (Figure 2A–D). Photographic and CT imaging examples documenting local responses are shown in Figure 2B–D. Crucially, when examining best systemic responses by immune related response criteria (25) at distant metastatic sites outside of the radiation portals, we observed one subject with a complete response, two with partial responses, one with disease stabilization, and one with progressive disease (Supplemental Table 1, Figure 2E–H). CT imaging examples of partial (Figure 2F–G) and complete responses (Figure 2H) of index lesions are depicted. Mirroring human cancer immunotherapy trials (1, 3), responses were rapid and robust with >80 – 100% reduction in the volume of index lesions (Figure 2E) and regression of even large bulky tumors (Figure 2F, H). Some of the partial responses consisted of a mixed response with regression of some lesions and growth or stability of others (Figure 2G). This type of mixed response has also been observed in human immunotherapy trials and is associated with a good prognosis (25). Thus, in canines with previously rapidly progressing disease the local response rate was 100% and the systemic response rate was 60%, with another 20% disease stabilization. Upon cessation of treatment in this trial, all dogs eventually had CT documented or clinical / symptomatic progression. No further treatment was provided beyond the brief treatment course outlined in the schema and assessment of longer administration, as is used in human trials, is needed.

Canines were monitored closely for toxicity with regular physical examinations and lab work. Importantly, the only adverse effects observed were mild mucositis and skin toxicity within the radiation portals that did not exceed what would be expected from palliative RT alone (Supplemental Table 1). These results demonstrate that this triple combination therapy can be safely administered resulting in significant anti-tumor effects in metastatic disease and validate the finding of our mouse studies in a model more representative of human cancer.

Addition of IDO blockade to RT + CpG transforms the immune suppressive tumor microenvironment

The primary rationale for adding 1MT to RT + CpG was our hypothesis that IDO mediated rebound immune suppression limited efficacy by maintaining Tregs and an immunosuppressive tumor microenvironment despite inflammatory signals. Clinical efficacy has been observed with RT + CpG but patients whose tumors induce Tregs are unlikely to respond (6). We examined the fate of immunosuppressive Tregs after the completion of therapy in mice and canines. In mice, Treg levels were maintained within the tumor after RT + CpG (Figure 3). The addition of 1MT significantly and substantially reduced the Treg subset of CD4+ T-cells within the tumor microenvironment but not in the periphery (Figure 3, supplemental Figure 2&3). The addition of 1MT resulted in a greater than four-fold decrease in intratumoral Tregs compared to RT + CpG alone 14 days post therapy (Figure

3A–B, p=0.02). This triple combination, but not immunotherapy alone (CpG +1MT), RT alone, or RT + CpG, significantly reduced Tregs compared to control mice (Figure 3A–B; control: 24.4% +/− 2.1% vs. RT + CpG + 1MT 6.2% +/− 2.2%; p<0.01). Similar results were seen if Tregs were analyzed as a percentage of total cells in the tumor (control: 0.093% +/− 0.072% vs. RT + CpG + 1MT 0.018% +/− 0.003%; p=0.07, data not shown). IL-6 induction after immunostimulatory therapies contributes to the reduction of Tregs. IDO can maintain Tregs in tumors by downregulating IL-6 (8). We observed a 9-fold increase in IL-6 expression within the tumor microenvironment after triple combination therapy (supplemental Figure 4, p=0.03). We also observed a significant three to four-fold increase in the CD4+/Treg ratio, which is a known indicator of immune status and prognosis (11, 30, 31), in RT + CpG + 1MT treated mice compared to tumor bearing control mice (p<0.01), CpG + 1MT treated mice (p<0.05), RT treated mice (p<0.01), and RT + CpG treated mice (p<0.01) (Figure 3C). The addition of 1MT provided no added benefit in terms of Treg reduction and improvement in the conventional CD4/Treg ratio in the dLN (supplemental Figure 2A–C), spleens (supplemental Figure 2D–F), or non-draining lymph nodes (data not shown). This is in contrast to the tumor, where the greatest Treg reductions were seen in the 1MT containing groups (CpG + 1MT and RT + CpG + 1MT, Figure 3A–C). Similar results were also seen at earlier time points (supplemental Figure 3). Thus, although 1MT was administered systemically, its primary action is within the tumor microenvironment where IDO is also up-regulated.

Informed by our murine studies, we examined the fate of Tregs in the tumors, dLN, and systemic circulation of canines receiving RT + CpG + 1MT (Figure 3 and supplemental Figure 2). When possible, tumor biopsy, tumor draining lymph node biopsy, and peripheral blood samples were obtained pre- and post-therapy. Peripheral blood was obtained from all dogs. A post-therapy tumor biopsy could not be obtained from one dog due to a complete response. Additionally, some dogs displayed massive tissue death in the post-treatment tumor biopsy samples limiting analyses. Lymph node biopsies could not be obtained from two dogs in which dLNs were not accessible with a minimally invasive procedure. Mirroring the results of our mouse studies, the percentage of tumor infiltrating Tregs was significantly reduced in all dogs post therapy with virtually no Tregs remaining in the tumor microenvironment post-therapy (Figure 3D–E, p=0.014). Conversely, in the three dLN samples we did not observe a statistically significant change in Tregs across the cohort with Tregs dropping substantially (3–4 fold) post-therapy in some dogs but increasing in others (supplemental Figure 2G). Also mirroring our mouse results, no significant change in peripheral Tregs was observed (supplemental Figure 2H). To confirm our results from flow cytometric analysis, immunofluorescence staining for FoxP3 expression in canines that had sufficient remaining biopsy samples was performed. Representative fields and quantification from a canine with Treg decreases in the tumor are depicted in Figure 3F–G confirming marked reduction in Foxp3+ cells following triple combination therapy. In the mouse tumor models, we also observed significant reductions in other immune suppressive factors in the tumor microenvironment. Tumor associated macrophages (TAMs) are known to play a critical suppressive role in the microenvironment of 4T1 tumors (32). Mirroring the reduction seen in Tregs only the RT + CpG + 1MT triple combination resulted in a statistically significant reduction of TAMs by nearly 5-fold compared to control (Figure 4A–

B; 18.4% +/− 10.3% vs. 3.8% +/− 1.5%; p<0.05). At baseline, intratumoral TAMs were M2 polarized as assessed by arginase to inducible nitric oxide ratio (data not shown). We next examined the expression of TGF-beta which both induces and is produced by Tregs and TAMs (reviewed in (33, 34)), is produced by IDO expressing dendritic cells (35) and is also known to block lymphocyte activation (36). All of the therapies reduced TGF-beta expression relative to control but this was most pronounced and most significant in the triple combination (Figure 4C, p<0.0001). Taken together, these studies indicate that this therapy reduces multiple immune suppressive factors and restores IL-6 signaling within the tumor microenvironment.

RT + CpG + 1-MT triple therapy anti-tumor effects are CD8+ T-cell dependent

We next examined the effects of this triple therapy on CD8+ T-cells and dendritic cells. The percentage of tumor infiltrating CD8+ T-cells (expressed as a percentage of total viable cells within the tumor) significantly increased from 0.68% in control mice to 2.71% 7 days after RT + CpG + 1MT (Figure 5A–B, p=0.02). The CD8+ T-cell/Treg ratio in the tumor was also increased by therapy from 6.3 to 21.7 (Figure 5C, p=0.0006). There were no changes in activation / functional / exhaustion markers such as PD-1, CD69 or IFN-gamma in the CD8+ T-cells after therapy but the majority of intratumoral CD8+ T-cells expressed these markers at baseline (data not shown). We also evaluated changes in tumor infiltrating CD8+ T-cells in treated canines. By flow cytometric analysis, there was a post-therapy increase in intratumoral CD8+ T-cells (as a percentage of all CD3+ intratumoral cells) in all three evaluable canines (Figure 5D–E). Overall, the frequency of intratumoral CD8+ T-cells doubled post-therapy which trended towards statistical significance (Figure 5D–E; 24% +/− 8.5% vs. 47.6% +/− 16.4%; p=0.06). IHC staining likewise demonstrated an increase in intratumoral CD8+ T-cells post-therapy (30 +/− 33 vs. 50 +/− 39 cells/HPF, Figure 5F–G, p=0.09). Mirroring our mouse studies therapy induced a significant increase in the CD8+ / Treg ratio (Figure 5H, p=0.014).

We tested the CD8 dependence of this therapy in mouse models. Depletion of CD8+ T-cells by intraperitoneal administration of anti-CD8 reduced the number of circulating CD8+ T-cells by >99% (supplemental Figure 5A–B). In mice depleted of CD8+ T-cells, we observed that the anti-tumor effects of RT + CpG + 1MT were significantly diminished. After treatment with the triple combination, tumors were more than tripled in size in CD8 depleted mice compared to those treated with control IgG (supplemental Figure 5C, 2066 mm^3 vs. 684 mm^3, p<0.0001). The survival benefit of the triple therapy was also significantly diminished in CD8 depleted mice (supplemental Figure 5D, p=0.03), indicating the critical role of CD8+ T-cells in the antitumor effects.

In addition to the effects of CD8+ T cells, we also evaluated dendritic cell (DC) activation and phenotypes following triple therapy. IDO expression has been linked to a tolerogenic DC phenotype, associated with decreased expression of CD80 and MHC II and increased TGF-beta production (35). No change in DC numbers or activation within dLNs was observed (data not shown). Recent data demonstrate that intratumoral DCs, although a minor population, play a critical role in anti-tumor T-cell responses (37, 38). Given that the major effects of this therapy occur in the tumor microenvironment we also examined DCs in the

tumor microenvironment. There was an increased number of activated DCs within treated tumors, with a four-fold increase in CD80 expressing DCs (supplemental Figure 6 A–C, p=0.02) and a near doubling of DC MHCII MFI compared to control mice (supplemental Figure 6 D–E, p=0.01).

Canine immunologic biomarkers

Finally, in three of the canine patients for which sufficient pre- and post-treatment tumor tissue was available we evaluated gene signatures by quantitative PCR (Figure 6). Based on our mouse data, we focused on expression of three immunosuppressive markers (IDO, TGF-beta, and FoxP3). Two of these patients demonstrated systemic partial responses and one had systemic progressive disease. Interestingly, in the two responders expression of all three immunosuppressive genes were markedly decreased post-therapy whereas all three were increased in the setting of progressive disease. These data suggest that this gene signature in the local tumor may represent a predictive biomarker for systemic response to this therapy and requires further evaluation in future studies. Overall, although hypothesis-generating in nature, these canine correlative immune analyses corroborate our mechanistic mouse data and provide rationale for further exploration of these immunologic endpoints in future studies.

Discussion

This is the first report of a novel immunotherapy strategy combining local RT + CpG with systemic IDO blockade. The primary purpose of this study was to examine whether IDO mediated rebound immune suppression after RT + CpG immunotherapy maintains an immunosuppressive microenvironment and limits efficacy. As hypothesized, RT + CpG paradoxically upregulated IDO expression, which we termed “rebound immune suppression”. Importantly, this immunotherapy-induced increase in IDO expression was also observed with other immunotherapies, suggesting that these mechanisms may have broader implications. Other studies also demonstrate the upregulation of IDO after inflammatory signals (20, 21). This rebound immune suppression suggests a physiologic regulatory mechanism whereby the immune system tempers responses in inflammatory settings to maintain homeostasis. The addition of IDO blockade decreased IDO activity and substantially increased local and systemic anti-tumor effects. Mechanistically, this therapy reduced multiple immune suppressive factors including Tregs, TAMs, and TGF-beta; increased intratumoral CD8+ T-cells; activated intratumoral DCs; and restored IL-6 signaling within the tumor microenvironment.

Although IDO blockade was administered systemically, the immunologic effects of IDO were most pronounced in the tumor microenvironment but limited in the tumor draining lymph nodes. This suggests that the immune re-activation is likely occurring directly within the tumor microenvironment and that this is sufficient to induce a systemic anti-tumor immune response. A recent report by Levy and colleagues indicates that reversal of immune suppression triggering an active immune response at a single site is sufficient to induce an effective systemic anti-tumor immune response (39). Our data are also corroborated by findings demonstrating that after checkpoint inhibition or IDO blockade little effect is seen

in the dLNs but there are marked effects on CD8+ T cells in the tumor (40). Likewise, recent data demonstrate that intratumoral DCs, although a minor population, play a critical role in anti-tumor T-cell responses (37, 38). Overall, our findings are in line with the published literature and support an emerging concept that augmenting a pre-existent but previously ineffective anti-tumor immune response directly within the local tumor micro-environment can serve as the nidus for a systemic response.

A principal finding of this study is the utility of RT in combination with immunotherapy. We observed no effect of the immunotherapies alone or in combination but robust effects in combination with RT (Figure 1). This synergy was seen in both the anti-tumor effects and the mechanistic immune changes induced by therapy. The reduction in tumor infiltrating Tregs and TAMs was only seen when RT was combined with immunotherapy (Figure 3). Likewise, the increase in tumor infiltrating CD8+ T-cells induced by RT + CpG + 1MT (Figure 5) was not seen with RT or immunotherapy alone (data not shown). These results add to the growing body of literature demonstrating the potent synergy of RT and immunotherapy.

The utility of mice to model human disease has recently been called into question (41). Mouse models provide an excellent platform for exploratory studies but often fail to adequately recapitulate treatment efficacy or toxicity in human clinical trials (42). The introduction of pre-translational confirmatory studies in a more robust model of human disease can help improve the efficiency of the translational pipeline by limiting human testing of therapies which are unlikely to be effective or tolerated. We tested our therapy in such a model by initiating a pilot veterinary clinical trial in companion canines with late stage metastatic spontaneous melanomas or sarcomas. These cancers arise, grow, and metastasize in the setting of an intact immune system and with patterns akin to human tumors (43). Canine immune systems are genetically and developmentally much more similar to humans than rodent models (44–47). Additionally, companion dogs share many environmental risk factors with their human owners. In dogs with rapidly progressive systemic disease our results demonstrated a significant response at the local RT treated primary tumor as well as response or disease stabilization in 80% of dogs at untreated sites of metastatic disease. This included substantial reductions of bulky pulmonary metastases which were well outside of the irradiated fields. We also observed significant changes in the immunosuppressive tumor micro-environment confirming the mechanistic data from our mouse models. Overall, the anti-tumor effects and mechanistic immunologic findings from our mouse models were paralleled in the canine clinical trial.

Immunotherapy can provide durable responses in a number of metastatic cancers (1–3). Unfortunately, most patients will fail to respond to these therapies and these treatments can induce significant toxicities. To increase response rates combinatorial strategies are being actively investigated. Recent clinical trials demonstrate that combining PD-1 and CTLA-4 checkpoint inhibitors can increase response rates in metastatic melanoma but are also accompanied by an equally marked increase in toxicity with 40% of patients responding but also 53% of patients experiencing grade 3 or 4 toxicities (48). These toxicities were attributed to the immune dysregulation induced by multiple checkpoint blockade. RT + CpG + 1MT employs immune stimulation in combination with blockade of immune suppression

limiting overlapping toxicity profiles and leaving multiple checkpoint pathways intact. We observed minimal toxicity with this regimen.

An area for future study is the assessment of longer courses of therapy. Treatment only lasted two weeks in mice and four weeks in canines. All of our canines eventually recurred after treatment discontinuation. Although robust responses were observed to this short treatment course most published immunotherapy strategies employ prolonged courses of therapy, and it is likely that prolonging the course of therapy in our models would further increase the magnitude and duration of response.

In summary, this study substantiates the power of combinatorial immunotherapy strategies and confirms that RT can be a potent partner for immunotherapy. Furthermore, it demonstrates that combinatorial strategies designed to minimize overlapping toxicity can be safe and effective. The correlative studies described here demonstrate the importance of post treatment tumor biopsies, which are rarely employed in human trials, to evaluate the immunologic changes induced by therapy and to further our understanding of the mechanistic underpinnings of therapy response and failure. Additionally, they suggest that IDO mediated rebound immune suppression may be a general mechanism of resistance to some immunotherapy strategies and that addition of IDO blockade may improve the effectiveness of such strategies. They demonstrate the feasibility of preclinical testing of immunotherapy in spontaneous canine malignancies as a pre-translational step in a model more reflective of human disease. Overall, these studies provide a strong rationale for clinical translation of this immunotherapy strategy to substantially improve the already documented efficacy of RT + CpG.

Supplementary Material

Refer to Web version on PubMed Central for supplementary material.

Acknowledgments

Financial Support: UC Davis CTSC K12 Scholar Program; NIH 2 KL2 RRO24144-06

American Cancer Society Institutional Research Grant; IRG-95-125-07

Amador Cancer Research Foundation; Christine and Helen Landgraf Award

NIH R01 CA 095572

NIH R01 CA 072669

NCI P30CA093373

We would like to acknowledge Weihong Ma, Shuaib Juma, Hong Chang, Hung Kieu, and Monja Metcalf for their technical support and Teri Guerrero for veterinary clinical trials support.

References

1. Brahmer JR, Tykodi SS, Chow LQ, Hwu WJ, Topalian SL, Hwu P, et al. Safety and activity of anti-PD-L1 antibody in patients with advanced cancer. N Engl J Med. 2012; 366:2455–2465. [PubMed: 22658128]

2. Hodi FS, O'Day SJ, McDermott DF, Weber RW, Sosman JA, Haanen JB, et al. Improved survival with ipilimumab in patients with metastatic melanoma. N Engl J Med. 2010; 363:711–723. [PubMed: 20525992]
3. Topalian SL, Hodi FS, Brahmer JR, Gettinger SN, Smith DC, McDermott DF, et al. Safety, activity, and immune correlates of anti-PD-1 antibody in cancer. N Engl J Med. 2012; 366:2443–2454. [PubMed: 22658127]
4. Formenti SC, Demaria S. Systemic effects of local radiotherapy. Lancet Oncol. 2009; 10:718–726. [PubMed: 19573801]
5. Milas L, Mason KA, Ariga H, Hunter N, Neal R, Valdecanas D, et al. CpG oligodeoxynucleotide enhances tumor response to radiation. Cancer Res. 2004; 64:5074–5077. [PubMed: 15289307]
6. Brody JD, Ai WZ, Czerwinski DK, Torchia JA, Levy M, Advani RH, et al. In situ vaccination with a TLR9 agonist induces systemic lymphoma regression: a phase I/II study. J Clin Oncol. 2010; 28:4324–4332. [PubMed: 20697067]
7. Kim YH, Gratzinger D, Harrison C, Brody JD, Czerwinski DK, Ai WZ, et al. In situ vaccination against mycosis fungoides by intratumoral injection of a TLR9 agonist combined with radiation: a phase 1/2 study. Blood. 2012; 119:355–363. [PubMed: 22045986]
8. Baban B, Chandler PR, Sharma MD, Pihkala J, Koni PA, Munn DH, et al. IDO activates regulatory T cells and blocks their conversion into Th17-like T cells. J Immunol. 2009; 183:2475–2483. [PubMed: 19635913]
9. Peng G, Guo Z, Kiniwa Y, Voo KS, Peng W, Fu T, et al. Toll-like receptor 8-mediated reversal of CD4+ regulatory T cell function. Science. 2005; 309:1380–1384. [PubMed: 16123302]
10. Wang Z, Zheng Y, Hou C, Yang L, Li X, Lin J, et al. DNA methylation impairs TLR9 induced Foxp3 expression by attenuating IRF-7 binding activity in fulminant type 1 diabetes. J Autoimmun. 2013; 41:50–59. [PubMed: 23490285]
11. Mitsuka K, Kawataki T, Satoh E, Asahara T, Horikoshi T, Kinouchi H. Expression of indoleamine 2,3-dioxygenase and correlation with pathological malignancy in gliomas. Neurosurgery. 2013; 72:1031–1038. discussion 1038–1039. [PubMed: 23426156]
12. Ye J, Liu H, Hu Y, Li P, Zhang G, Li Y. Tumoral indoleamine 2,3-dioxygenase expression predicts poor outcome in laryngeal squamous cell carcinoma. Virchows Arch. 2013; 462:73–81. [PubMed: 23179760]
13. Uyttenhove C, Pilotte L, Theate I, Stroobant V, Colau D, Parmentier N, et al. Evidence for a tumoral immune resistance mechanism based on tryptophan degradation by indoleamine 2,3-dioxygenase. Nat Med. 2003; 9:1269–1274. [PubMed: 14502282]
14. Munn DH, Mellor AL. Indoleamine 2,3-dioxygenase and tumor-induced tolerance. J Clin Invest. 2007; 117:1147–1154. [PubMed: 17476344]
15. Sharma MD, Baban B, Chandler P, Hou DY, Singh N, Yagita H, et al. Plasmacytoid dendritic cells from mouse tumor-draining lymph nodes directly activate mature Tregs via indoleamine 2,3-dioxygenase. J Clin Invest. 2007; 117:2570–2582. [PubMed: 17710230]
16. Sharma MD, Hou DY, Liu Y, Koni PA, Metz R, Chandler P, et al. Indoleamine 2,3-dioxygenase controls conversion of Foxp3+ Tregs to TH17-like cells in tumor-draining lymph nodes. Blood. 2009; 113:6102–6111. [PubMed: 19366986]
17. Chen W, Liang X, Peterson AJ, Munn DH, Blazar BR. The indoleamine 2,3-dioxygenase pathway is essential for human plasmacytoid dendritic cell-induced adaptive T regulatory cell generation. J Immunol. 2008; 181:5396–5404. [PubMed: 18832696]
18. Yan Y, Zhang GX, Gran B, Fallarino F, Yu S, Li H, et al. IDO upregulates regulatory T cells via tryptophan catabolite and suppresses encephalitogenic T cell responses in experimental autoimmune encephalomyelitis. J Immunol. 2010; 185:5953–5961. [PubMed: 20944000]
19. Mellor AL, Munn DH. IDO expression by dendritic cells: tolerance and tryptophan catabolism. Nat Rev Immunol. 2004; 4:762–774. [PubMed: 15459668]
20. Mellor AL, Baban B, Chandler PR, Manlapat A, Kahler DJ, Munn DH. Cutting edge: CpG oligonucleotides induce splenic CD19+ dendritic cells to acquire potent indoleamine 2,3-dioxygenase-dependent T cell regulatory functions via IFN Type 1 signaling. J Immunol. 2005; 175:5601–5605. [PubMed: 16237046]

21. Von Bubnoff D, Scheler M, Wilms H, Fimmers R, Bieber T. Identification of IDO-positive and IDO-negative human dendritic cells after activation by various proinflammatory stimuli. J Immunol. 2011; 186:6701–6709. [PubMed: 21543643]
22. Hou DY, Muller AJ, Sharma MD, DuHadaway J, Banerjee T, Johnson M, et al. Inhibition of indoleamine 2,3-dioxygenase in dendritic cells by stereoisomers of 1-methyl-tryptophan correlates with antitumor responses. Cancer Res. 2007; 67:792–801. [PubMed: 17234791]
23. Murphy WJ, Welniak L, Back T, Hixon J, Subleski J, Seki N, et al. Synergistic anti-tumor responses after administration of agonistic antibodies to CD40 and IL-2: coordination of dendritic and CD8+ cell responses. J Immunol. 2003; 170:2727–2733. [PubMed: 12594303]
24. Perks JR, Lucero S, Monjazeb AM, Li JJ. Anthropomorphic Phantoms for Confirmation of Linear Accelerator-Based Small Animal Irradiation. Cureus. 2015; 7:e254. [PubMed: 26180678]
25. Wolchok JD, Hoos A, O'Day S, Weber JS, Hamid O, Lebbe C, et al. Guidelines for the evaluation of immune therapy activity in solid tumors: immune-related response criteria. Clin Cancer Res. 2009; 15:7412–7420. [PubMed: 19934295]
26. Ladue T, Klein MK. Veterinary Radiation Therapy Oncology G. Toxicity criteria of the veterinary radiation therapy oncology group. Vet Radiol Ultrasound. 2001; 42:475–476. [PubMed: 11678573]
27. Aslakson CJ, Miller FR. Selective events in the metastatic process defined by analysis of the sequential dissemination of subpopulations of a mouse mammary tumor. Cancer Res. 1992; 52:1399–1405. [PubMed: 1540948]
28. Jia L, Schweikart K, Tomaszewski J, Page JG, Noker PE, Buhrow SA, et al. Toxicology and pharmacokinetics of 1-methyl-d-tryptophan: absence of toxicity due to saturating absorption. Food Chem Toxicol. 2008; 46:203–211. [PubMed: 17868966]
29. Proulx DR, Ruslander DM, Dodge RK, Hauck ML, Williams LE, Horn B, et al. A retrospective analysis of 140 dogs with oral melanoma treated with external beam radiation. Vet Radiol Ultrasound. 2003; 44:352–359. [PubMed: 12816381]
30. Koyama K, Kagamu H, Miura S, Hiura T, Miyabayashi T, Itoh R, et al. Reciprocal CD4+ T-cell balance of effector CD62Llow CD4+ and CD62LhighCD25+ CD4+ regulatory T cells in small cell lung cancer reflects disease stage. Clin Cancer Res. 2008; 14:6770–6779. [PubMed: 18980970]
31. Sinicrope FA, Rego RL, Ansell SM, Knutson KL, Foster NR, Sargent DJ. Intraepithelial effector (CD3+)/regulatory (FoxP3+) T-cell ratio predicts a clinical outcome of human colon carcinoma. Gastroenterology. 2009; 137:1270–1279. [PubMed: 19577568]
32. Luo Y, Zhou H, Krueger J, Kaplan C, Lee SH, Dolman C, et al. Targeting tumor-associated macrophages as a novel strategy against breast cancer. J Clin Invest. 2006; 116:2132–2141. [PubMed: 16862213]
33. Chen W, Konkel JE. TGF-beta and 'adaptive' Foxp3(+) regulatory T cells. J Mol Cell Biol. 2010; 2:30–36. [PubMed: 19648226]
34. Teicher BA. Transforming growth factor-beta and the immune response to malignant disease. Clin Cancer Res. 2007; 13:6247–6251. [PubMed: 17975134]
35. Yang J, Yang Y, Fan H, Zou H. Tolerogenic splenic IDO (+) dendritic cells from the mice treated with induced-Treg cells suppress collagen-induced arthritis. J Immunol Res. 2014; 2014:831054. [PubMed: 25405209]
36. Stephen TL, Rutkowski MR, Allegrezza MJ, Perales-Puchalt A, Tesone AJ, Svoronos N, et al. Transforming growth factor beta-mediated suppression of antitumor T cells requires FoxP1 transcription factor expression. Immunity. 2014; 41:427–439. [PubMed: 25238097]
37. Broz ML, Binnewies M, Boldajipour B, Nelson AE, Pollack JL, Erle DJ, et al. Dissecting the tumor myeloid compartment reveals rare activating antigen-presenting cells critical for T cell immunity. Cancer Cell. 2014; 26:638–652. [PubMed: 25446897]
38. Ruffell B, Chang-Strachan D, Chan V, Rosenbusch A, Ho CM, Pryer N, et al. Macrophage IL-10 blocks CD8+ T cell-dependent responses to chemotherapy by suppressing IL-12 expression in intratumoral dendritic cells. Cancer Cell. 2014; 26:623–637. [PubMed: 25446896]

39. Marabelle A, Kohrt H, Sagiv-Barfi I, Ajami B, Axtell RC, Zhou G, et al. Depleting tumor-specific Tregs at a single site eradicates disseminated tumors. J Clin Invest. 2013; 123:2447–2463. [PubMed: 23728179]

40. Spranger S, Koblish HK, Horton B, Scherle PA, Newton R, Gajewski TF. Mechanism of tumor rejection with doublets of CTLA-4, PD-1/PD-L1, or IDO blockade involves restored IL-2 production and proliferation of CD8(+) T cells directly within the tumor microenvironment. J Immunother Cancer. 2014; 2:3. [PubMed: 24829760]

41. Seok J, Warren HS, Cuenca AG, Mindrinos MN, Baker HV, Xu W, et al. Genomic responses in mouse models poorly mimic human inflammatory diseases. Proc Natl Acad Sci U S A. 2013; 110:3507–3512. [PubMed: 23401516]

42. Voskoglou-Nomikos T, Pater JL, Seymour L. Clinical predictive value of the in vitro cell line, human xenograft, and mouse allograft preclinical cancer models. Clin Cancer Res. 2003; 9:4227–4239. [PubMed: 14519650]

43. Felsburg PJ. Overview of immune system development in the dog: comparison with humans. Hum Exp Toxicol. 2002; 21:487–492. [PubMed: 12458905]

44. Gu YC, Bauer TR Jr, Ackermann MR, Smith CW, Kehrli ME Jr, Starost MF, et al. The genetic immunodeficiency disease, leukocyte adhesion deficiency, in humans, dogs, cattle, and mice. Comp Med. 2004; 54:363–372. [PubMed: 15357315]

45. Holsapple MP, West LJ, Landreth KS. Species comparison of anatomical and functional immune system development. Birth Defects Res B Dev Reprod Toxicol. 2003; 68:321–334. [PubMed: 14666995]

46. Govindaraj RG, Manavalan B, Basith S, Choi S. Comparative analysis of species-specific ligand recognition in Toll-like receptor 8 signaling: a hypothesis. PLoS One. 2011; 6:e25118. [PubMed: 21949866]

47. Liu J, Xu C, Hsu LC, Luo Y, Xiang R, Chuang TH. A five-amino-acid motif in the undefined region of the TLR8 ectodomain is required for species-specific ligand recognition. Mol Immunol. 2010; 47:1083–1090. [PubMed: 20004021]

48. Wolchok JD, Kluger H, Callahan MK, Postow MA, Rizvi NA, Lesokhin AM, et al. Nivolumab plus ipilimumab in advanced melanoma. N Engl J Med. 2013; 369:122–133. [PubMed: 23724867]

Statement of Translational Relevance

Cancer immunotherapy consisting of radiotherapy in combination with intratumoral CpG has proven highly effective in some patients and additional trials are ongoing. Unfortunately, most patient fail to respond to this therapy. In this report we demonstrate that the effectiveness of this therapy may be limited by upregulation of IDO in the tumor microenvironment in response to the therapy itself. IDO upregulation maintains immune suppression within the tumor and limits an effective anti-tumor immune response. Addition of IDO blockade to this therapy reverses intra-tumoral immune suppression and substantially improves local and systemic efficacy without any apparent increase in toxicity. Given the use of IDO inhibitors and radiotherapy + CpG in clinical trials, and that this triple therapy has now been tested in large animal models, this therapy is ready for clinical translation.

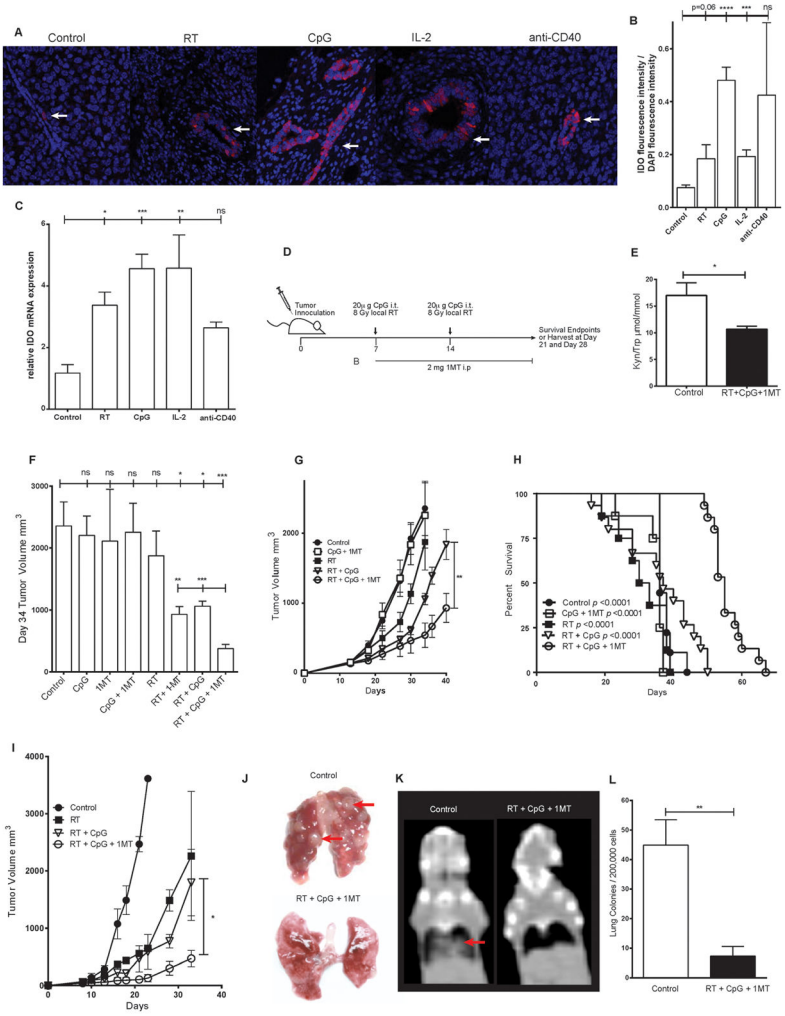

Figure 1. 1MT limits radiation + CpG induced IDO up-regulation and improves therapeutic efficacy

Expression of IDO in control or treated 4T1 tumors by immunofluorescence (A, B) or qPCR (C). IDO + cells stain bright pink and nuclei are counterstained by DAPI, white arrows indicate examples of positive staining cells. Balb/c mice bearing orthotopic 4T1 breast tumors or C57/BL6 mice bearing B16 melanoma tumors were treated as outlined in the schema (D). IDO enzymatic activity in 4T1 tumor bearing mice as measured by serum kynurenine to tryptophan ratio (E). 4T1 tumor growth (F,G) and tumor bearing mouse survival (H). B16 melanoma tumor growth (I). Lung metastases in orthotopic 4T1 bearing mice as assessed by gross examination (J), computed tomography (K), and lung colony forming assay (L). Red arrows indicate examples of lung metastases. n=3–4 mice per group for correlative studies and n=6–10 mice per group for tumor growth studies and survival studies. Bar graphs represent mean +/− standard error of mean. Results analyzed by one-way ANOVA, student's t-test, or kaplan-meier analysis between the indicated groups (* $p < 0.05$, ** $p < 0.01$, *** $p < 0.001$).

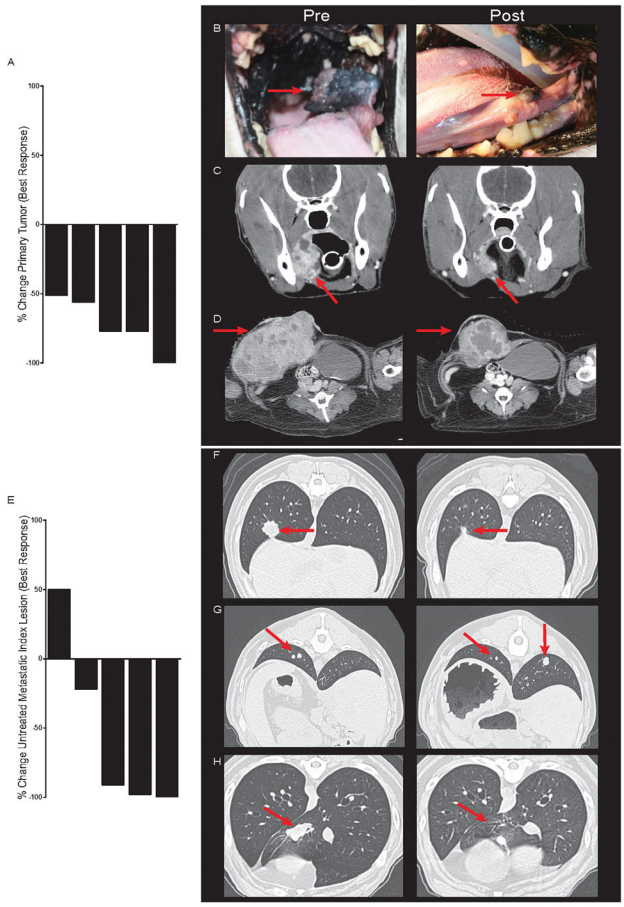

Figure 2. Efficacy of radiation + CpG + 1MT in a canine clinical trial

Therapeutic response of local irradiated tumors (**A-D**) and untreated metastatic lesions (**E–H**) in a canine clinical trial are depicted. Waterfall plot of best response at the primary treated tumor (**A**). Photographs (**B**) and computed tomography (**C**) depicting response of a melanoma of the buccal mucosa. Computed tomography depicting response of an abdominal wall sarcoma (**D**). Waterfall plot of best response at untreated metastatic index lesions (**E**). Computed tomography demonstrating a partial response (**F**), mixed response (**G**), and complete response (**H**) of metastatic pulmonary index lesions.

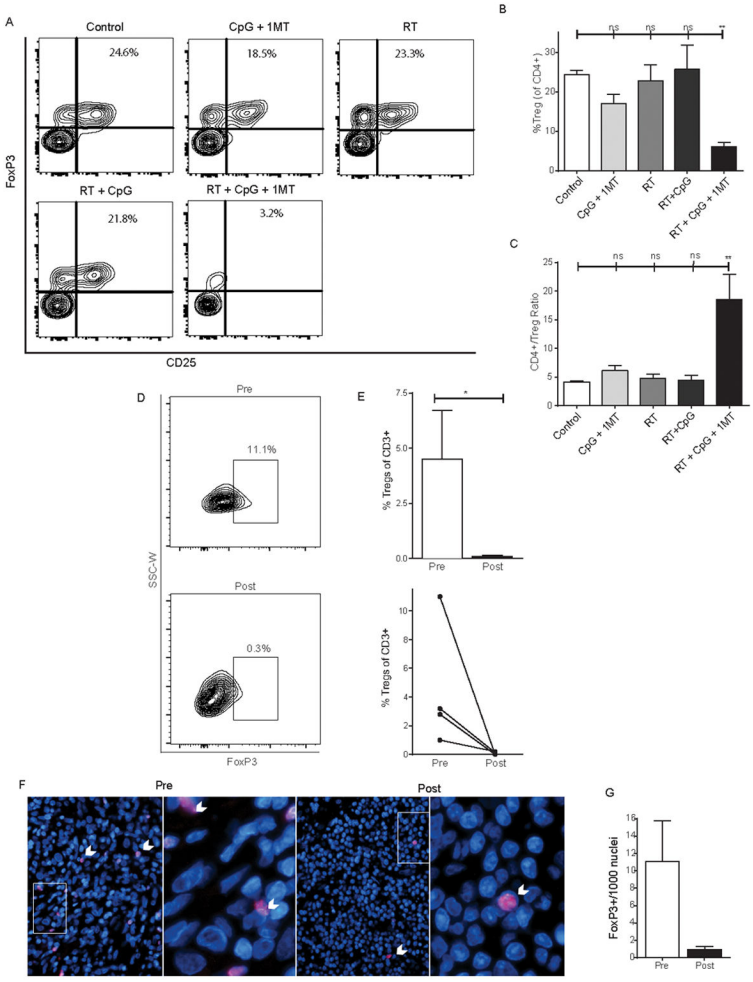

Figure 3. Radiation + CpG + 1MT reduces intratumoral regulatory CD4+ T-cells in mice and canines

Day 28 levels of tumor infiltrating regulatory CD4+ T-cells as assessed by flow cytometry and immunofluorescence in 4T1 bearing mice (**A–C**) or canine patients (**D–G**) treated with RT + CpG + 1MT. Representative flow cytometry contour plots demonstrating staining of intratumoral CD4+ cells for FoxP3 and CD25 (**A**). Flow cytometry data represented as a bar graph expressed as %Treg (CD4+,CD25+,FoxP3+) of CD4+ cells (**B**). Bar graph representation of CD4+ to Treg ratio as measured by flow cytometry (**C**). Representative flow cytometry plots demonstrating staining of canine intratumoral CD4+ cells for FoxP3 pre- and post- RT + CpG + 1MT therapy (**D**). Bar graph representation of intratumoral Tregs pre- and post-therapy expressed as a percentage of CD3+ cells in four canine patients as assessed by flow cytometry (**E**). Line graph demonstrates changes in Treg levels in individual patients as assessed by flow cytometry (**E**). Immuno-fluorescent staining of canine tumor samples for FoxP3 (**F**). FoxP3 + cells stain bright pink and nuclei are counterstained by DAPI, white arrows point out examples of positive staining cells. Bar graph quantification of intratumoral FoxP3 positive cells (**G**). n=3–4 mice per group and four canines patients. Bar graphs represent mean +/− standard error of mean. Results

analyzed by one-way ANOVA or student's t-test between the indicated groups (* $p < 0.05$, ** $p < 0.01$).

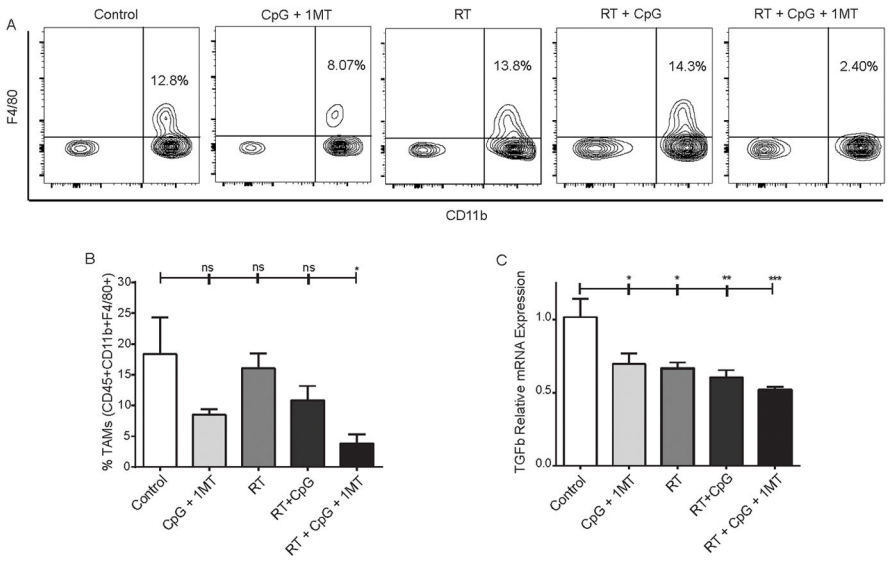

Figure 4. Radiation + CpG + 1MT reduces tumor associated macrophages

Levels of intratumoral CD45+CD11b+F4/80+ macrophages as assessed by flow cytometry in 4T1 bearing mice (**A–B**). Representative flow cytometry contour plots demonstrating staining of intratumoral CD45+ cells for F4/80 and CD11b (**A**). Flow cytometry data represented as a bar graph expressed as % tumor associated macrophages of all CD45+ cells (**B**). Bar graph representation of intratumoral transforming growth factor beta mRNA as assessed by qPCR (**C**). n=3–4 mice per group. Bar graphs represent mean +/− standard error of mean. Results analyzed by one-way ANOVA between the indicated groups (* $p < 0.05$, ** $p < 0.01$, *** $p < 0.001$, **** $p < 0.0001$).

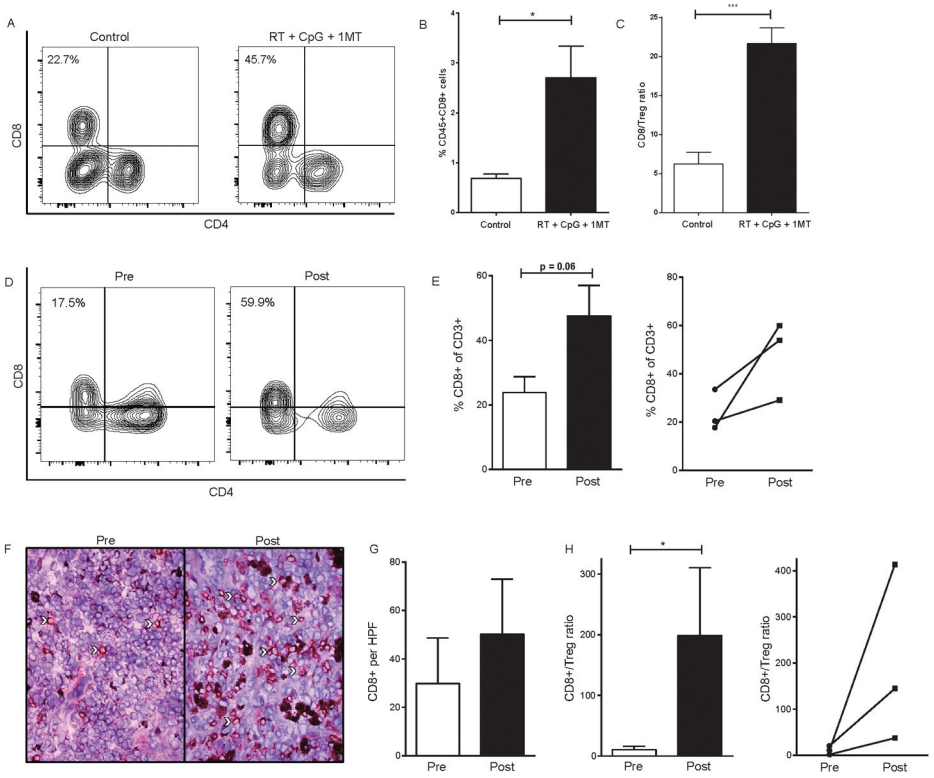

Figure 5. Radiation + CpG + 1MT increases tumor infiltrating CD8+ T cells in mice and canines

Representative flow cytometry contour plots demonstrating staining of tumor infiltrating CD45+CD3+ cells for CD8 and CD4 (**A**). Flow cytometry data of tumor infiltrating CD8+ T-cells represented as a bar graph expressed as % CD8+ cells of all CD45+ cells (**B**). CD8+ T cell to regulatory T cell ratio as determined by flow cytometry (**C**). Levels of tumor infiltrating CD8+ T cells as assessed by flow cytometry in canine tumors (**D-E**). Representative flow cytometry contour plots demonstrating staining of canine intratumoral CD8+ and CD4+ T cells pre- and post- RT + CpG + 1MT therapy (**D**). Bar graph representation of intratumoral CD8+ T cells expressed as a percentage of CD3+ cells in three canine patients as assessed by flow cytometry (**E**). Line graph demonstrates changes in Treg levels in individual patients as assessed by flow cytometry (**E**). Immunohistochemical staining with tumor infiltrating CD8+ T-cells stained in red, white arrows point out examples of positive staining cells (**F**). Bar graph quantification of intratumoral CD8 positive cells (**G**). CD8+ T cell to regulatory T cell ratio as determined by flow cytometry (**H**). Line graph demonstrates changes in CD8+ T cell to regulatory T cell ratio in individual patients pre- to post-treatment (**H**). n=3–4 mice per group and three canines patients. Bar graphs represent mean +/− standard error of mean. Results analyzed by student's t-test (* $p < 0.05$, ** $p < 0.01$, *** $p < 0.001$, **** $p < 0.0001$).

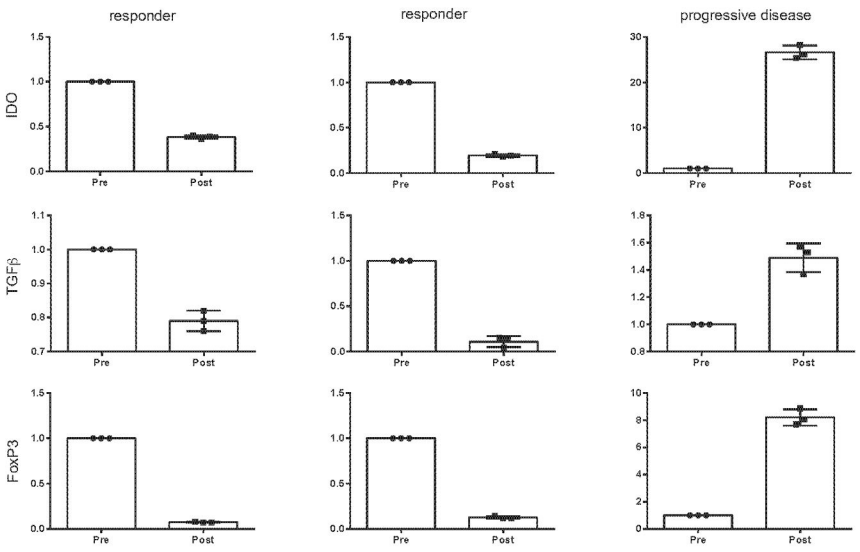

Figure 6. Intratumoral expression of immunosuppressive molecules as a gene signature of systemic anti-tumor immune response in canines treated with radiation + CpG + 1MT

Sufficient pre- and post-therapy tumor tissue was available for further analysis in three canines: two responders and one with progressive disease. Expression of the immunosuppressive molecules IDO, TGF beta, and FoxP3 was assessed by qPCR and results are expressed relative mRNA expression of technical triplicates. Bar graphs represent mean +/− standard error of mean.